

Validation of the ICESat vegetation product using crown-area-weighted mean height derived using crown delineation with discrete return lidar data

Yong Pang, Michael Lefsky, Hans-Erik Andersen, Mary Ellen Miller, and Kirk Sherrill

Abstract. The Geoscience Laser Altimeter System (GLAS), a spaceborne light detection and ranging (lidar) sensor, has acquired over 250 million lidar observations over forests globally, an unprecedented dataset of vegetation height information. To be useful, GLAS must be calibrated to measurements of height used in forestry inventory and ecology. Airborne discrete return lidar (DRL) can characterize vegetation and terrain surfaces in detail, but its utility as calibration data for GLAS is limited by the lack of a direct relationship between the canopy height measurements collected by airborne and spaceborne lidar systems and coincident field data. We demonstrate that it is possible to use DRL to directly estimate the crown-area-weighted mean height (H_{cw}), which is conceptually and quantitatively similar to the Lorey's height, which is calculated from forest inventory data, and can be used to calibrate GLAS without the use of field data. For a dataset from five sites in western North America, the two indices of height (H_{cw} from DRL and Lorey's from forest inventory) are directly related ($r^2 = 0.76$; RMSE of 3.8 m; intercept and slope of 0.8 m and 0.98, respectively). We derived a relationship between the DRL-derived H_{cw} and height information from coincident GLAS waveforms; the resulting equation explained 69% of variance, with an RMSE of 6.2 m.

Résumé. Le système GLAS (« Geoscience Laser Altimeter System »), un capteur lidar (« light detection and ranging ») satellitaire, a acquis plus de 250 millions d'observations lidar au-dessus des forêts à l'échelle du globe, constituant ainsi un ensemble inédit de données d'information sur les hauteurs. Pour être utile, le capteur GLAS doit être étalonné par rapport à des mesures de hauteur utilisées dans les inventaires forestiers et en écologie. Les données lidar aéroporté à retours discrets (DRL) permettent de caractériser les surfaces de végétation et de terrain en détail, mais leur utilité comme données d'étalonnage pour GLAS est limitée par l'absence de relation directe entre ces données et les estimations de hauteur recueillies sur le terrain. Nous faisons la démonstration qu'il est possible d'utiliser les données DRL pour estimer directement la hauteur moyenne pondérée de la superficie de la cime (H_{cw}), qui est conceptuellement et quantitativement similaire à la hauteur moyenne de Lorey qui elle est calculée à partir des données d'inventaire forestier et qui peut être utilisée pour étalonner le capteur GLAS sans avoir recours à des données de terrain. Dans le cas des ensembles de données de cinq sites situés dans l'ouest de l'Amérique du Nord, les deux indices de hauteur (H_{cw} calculée à partir des données DRL et la hauteur moyenne de Lorey calculée à partir des données d'inventaire forestier) sont directement reliés (r^2 de 0,76, RMSE de 3,8 m, intercept et pente de 0,8 m et 0,98 respectivement). Nous avons dérivé une relation entre la hauteur H_{cw} dérivée des données DRL et l'information sur la hauteur dérivée des formes d'onde correspondantes de GLAS; l'équation résultante a permis d'expliquer 69 % de la variance avec une valeur RMSE de 6,2 m.
[Traduit par la Rédaction]

Introduction

The Geoscience Laser Altimeter System (GLAS) on board the Ice, Cloud, and Land Elevation Satellite (ICESat) is a waveform-sampling light detection and ranging (lidar) sensor

that emits short-duration (5 ns) laser pulses towards the land surface and records the echo of those pulses as they reflect off the ground surface. When that surface is vegetated, the return echoes, or waveforms, record the vertical distribution of vegetation and terrain surfaces within the area illuminated by

Received 19 February 2008. Accepted 17 November 2008. Published on the *Canadian Journal of Remote Sensing* Web site at <http://pubs.nrc-cnrc.gc.ca/cjrs> on 19 December 2008.

Y. Pang.¹ Center for Ecological Applications of Lidar, College of Natural Resources, Colorado State University, Fort Collins, CO 80523, USA; and Institute of Forest Resource and Information Technology, Chinese Academy of Forestry, Beijing 100091, China.

M. Lefsky, M.E. Miller, and K. Sherrill. Center for Ecological Applications of Lidar, College of Natural Resources, Colorado State University, Fort Collins, CO 80523, USA.

H.-E. Andersen. Forest Inventory and Analysis, USDA Forest Service PNW Research Station, Anchorage Forestry Sciences Laboratory, Anchorage, AK 99503, USA.

¹Corresponding author (e-mail: caf.pang@gmail.com).

the laser (the footprint). GLAS has acquired over 250 million individual lidar observations over forest regions globally, an unprecedented dataset of vegetation heights. Accurate vegetation heights have been retrieved from these measurements (Harding and Carabajal, 2005; Lefsky et al., 2005; 2007; Sun et al., 2008). Lefsky et al. (2005) showed that these estimates of height could, as with other lidar estimates of height, accurately estimate aboveground biomass as well.

The GLAS laser footprint is elliptical and varies in size as a function of laser operating conditions. Its nominal footprint diameter is 70 m but may vary between 52 and 105 m (Zwally et al., 2002; nsidc.org/data/icesat/glas_laser_ops_attrib.pdf). A footprint of this size may contain hundreds of trees. It would be prohibitively expensive to collect all the field data that would be required to develop the relationships between GLAS waveform extent and forest canopy height needed to create a global product. Airborne discrete return lidar (DRL) can provide highly detailed canopy height measurements, where the data represent 3-D coordinates of reflections from small diameter (<0.5 m) laser pulses collected at a high density (>1 pulse/m²). Therefore, DRL has the potential to accurately and precisely characterize the vegetation and terrain surfaces within the footprint of a GLAS shot. The detail and precision of airborne DRL far exceeds the capabilities of fieldwork to characterize vegetation at the scales and quantities required. Airborne DRL is becoming an operationally mature remote sensing technology for forest assessment, and high-density airborne DRL data are becoming generally available for many forested sites worldwide (Naesset, 2004; Stoker et al., 2007). A general method for deriving an index of average tree height from these datasets, using a minimum of ancillary data, would allow the widespread use of these data for calibration of GLAS data, and for other sources of remotely sensed data used to estimate forest structure generally (e.g., synthetic aperture radar).

High-density DRL data can be used to estimate two classes of height index. The first represents the bulk properties of discrete returns (Magnussen and Boudewyn, 1998; Naesset, 2004), including indices such as the percent of returns from the forest canopy, or the 50th or 90th percentile return height. The second class of index includes those related to the properties of individual trees such as their location, height, crown size, and crown length (Hyypä et al., 2001; Andersen et al., 2001; Popescu et al., 2003; Persson et al., 2002; Morsdorf et al., 2004; Falkowski et al., 2006; Chen et al., 2006; Solberg et al., 2006).

Although the first class of index can be estimated with fewer processing steps, both classes cannot be measured directly in the field and are most often calibrated using heights from coincident field inventory. In contrast, a robust method of individual tree delineation could, once validated, be used without the need for coincident field data. This is especially so if the ultimate goal is to estimate plot-level summaries of tree height.

Algorithms for the delineation of individual trees (**Table 1**) were originally developed for use with high-resolution optical remote sensing imagery; these algorithms have been extended

to operate on lidar-derived canopy height models (CHM; the uppermost elevation surface derived from DRL data). Common features of existing methods for individual crown delineation are creating the CHM, locating trees, and defining a segment around identified trees to identify crown boundaries.

Many canopy segmentation approaches combine several crown delineation techniques and processes, for example, a local-maxima approach is used to identify tree locations and a region-growing or a morphological watershed method is used to delineate the crown boundaries.

Most algorithms require a local relationship between tree height and crown size as prior knowledge that is used to search for a local maximum (Hyypä et al., 2001), determine the size of a circular search window (Popescu et al., 2003), justify template scale (Brandtberg et al., 2003), find tree-top markers (Chen et al., 2006), or some combination of these. The pouring algorithm proposed by Persson et al. (2002) and Koch et al. (2006) avoids the need for prior information by detecting local maxima at different scales and varying smoothing intensities. However, a range of possible scales (three scales used in Persson et al., 2002) and a threshold for height classes (20 m was used in Koch et al., 2006) were still needed. The spatial wavelet analysis (SWA) method does not require prior information either, but it has only been assessed in open stands (Falkowski et al., 2006). After crown delineation, a circle (Morsdorf et al., 2004), average radius along cardinal directions (Solberg et al., 2006), or ray algorithm (Koch et al., 2006) can be used to estimate crown size. All of these algorithms require prior knowledge of local forest sites or are adapted to specific forest types. To use DRL data to evaluate height in a variety of forests, a self-calibrating crown delineation and tree height estimation technique is needed. In this paper, we provide the outline of such an approach and a validation for the limited goal of estimating plot-level summaries of individual tree attributes.

The objectives of this paper are as follows: (i) demonstrate that crown-area-weighted height can be estimated from discrete return lidar data using an automated crown-segmentation method, and that those estimates are a satisfactory estimate of Lorey's height estimated in the field at five coniferous sites in western North America; and (ii) demonstrate the ability to validate the ICESat vegetation product using crown-area-weighted height derived from coincident discrete-return lidar data at four coniferous sites in western North America. Realization of these individual objectives results in a repeatable method for creating estimates of crown-area-weighted height from GLAS data that can be applied anywhere coincident discrete return data are available.

Methods

Study area and field data

Data from a total of seven coniferous forest sites in western North America are considered in this work: two in California, two in Colorado, and one each in Alaska, Washington, and

Table 1. Methods for individual tree crown delineation.

Algorithm	Reference study	Location	Forest type	Lidar system	Lidar point density (points/m ²)	Accuracy ^a
Pouring–watershed	Persson et al., 2002	Southern Sweden	Conifer	TopEye	>4	0.98 (0.63 m); 0.58 (0.61 m)
Pouring–watershed	Koch et al. 2006	Southwest Germany	Conifer and deciduous	TopoSys	5–10	61.7% crowns correct or satisfactory
Pouring–watershed	Chen et al., 2006	California, USA	Blue oak	ALTM	9.5	Crown area 61.3%–68.2%
Region growing	Hyypä et al., 2001	Southern Finland	Conifer	TopoSys	8–10	Standard error 1.8 m (9.9%)
Region growing	Solberg et al., 2006	Southeastern Norway	Conifer	ALTM	5	0.86 (1.4 m); 0.52 (1.1 m)
Scale-space theory	Brandtberg et al., 2003	Eastern USA	Deciduous	TopEye	15	68% (1.1 m); na
Curve fitting	Popescu et al., 2003	Southeastern USA	Conifer and deciduous	AeroScan	1.35	na; 0.62 (1.36 m)
Three-dimensional clustering	Morsdorf et al., 2004	Switzerland	Conifer	TopoSys	>10	0.92 (0.61 m); 0.20 (0.47 m)
Spatial wavelet	Falkowski et al., 2006	Idaho, USA	Conifer	ALS40	na	0.94 (2.64 m); 0.74 (1.35 m)

^aUnless noted otherwise, the first set of values is the accuracy for tree height R_h^2 , with RMSE in parentheses, and the second set of values is the accuracy for crown diameter R_c^2 , with RMSE in parentheses. na, not available.

Table 2. Study area characteristics.

Study area	No. of GLAS shots	No. of field plots	Lidar system ^a	Lidar density (points/m ²)	GLAS period ^b	Acquisition date	Location
Bonanza Creek ^c	32	—	3070	2.0	L3F	May 2005	Alaska
Fraser Experimental Forest ^d	—	48	2025, 2050	2.4	—	October 2005	Front Range, Colorado
Glacier Lakes Ecosystem Experiments site (Glees) ^d	—	48	2025, 2050	2.4	—	July 2006	Southern Wyoming
Mission Creek ^e	22	66	3070	5.0	L3F	August 2004	East Cascades, Washington State
Niwot Ridge Long Term Ecological Research ^d	—	48	2025, 2050	1.6	—	October 2005	Front Range, Colorado
San Bernardino ^c	9	—	3100	7.0	L3F	August 2005	Southern California
Tahoe ^e	358	32	2050	3.5	L2B, L3D, L3E, L3F	September 2005	Northern California

^aAll lidar data were collected with the OPTTECH ALTM lidar system.

^bDate for each GLAS period as follows: L2B, February–March 2004; L3D, October–November 2005; L3E, February–March 2006; L3F, May–June 2006.

^cUsed to calibrate GLAS estimates of height.

^dUsed to compare Lorey's height from field measurement and crown-area-weighted height from airborne lidar data.

^eUsed to calibrate GLAS estimates of height and to compare Lorey's height from field measurement and crown-area-weighted height from airborne lidar data.

Wyoming. Each site supplied data for one or both of two sets of analyses: (i) verification of the crown delineation technique, and (ii) analysis of the relationship between heights derived from the crown delineation technique and from GLAS waveforms (see **Table 2**).

Bonanza Creek Experimental Forest (64.75°N, 148.27°W) is located approximately 20 km southwest of Fairbanks, Alaska, and contains a variety of upland and lowland boreal forest types characteristic of this region of interior Alaska. This forest has an elevational gradient ranging from 120 m at the Tanana

floodplain to 470 m at ridge crest. Well-drained, south-facing upland sites are primarily composed of aspen (*Populus tremuloides*), paper birch (*Betula papyrifera*), and white spruce (*Picea glauca*), and north-facing sites and poorly drained lowlands are occupied by slow-growing black spruce (*Picea mariana*). On permafrost-free, alluvial sites within the floodplain, balsam poplar (*Populus balsamifera*) and white spruce are the predominant species, and black spruce is commonly found in boggy areas of the floodplain where permafrost is present (www.lter.uaf.edu/bcef/vegetation.cfm).

DRL data from Bonanza Creek were used to calibrate GLAS estimates of height.

The Mission Creek study area (47.46°N, 120.52°W) in Wenatchee National Forest is located in the Mission Creek drainage within the eastern Cascade Mountains of Washington State. This area is mountainous, with slopes in forested areas ranging from 0 to 50° across a range of aspects, and elevations varying from 900 m at the Wenatchee River to 4500 m in the mountains. Dry mixed-conifer forests in this area are composed primarily of Douglas fir (*Pseudotsuga menziesii*), ponderosa pine (*Pinus ponderosa*), grand fir (*Abies grandis*), western larch (*Larix occidentalis*), and various shrub species. Field data from Mission Creek were used to verify the ability of the crown delineation algorithm to map individual stems and compare Lorey's and crown-area-weighted height, and DRL was used to calibrate GLAS estimates of height.

The Mission Creek site has 20 m × 50 m plots with stem-mapped individual tree data that were used to evaluate lidar estimates of individual tree parameters. Tree species, diameter at breast height (dbh), height, crown class, and tree coordinates were recorded for all trees greater than 1 cm, and each tree location was mapped using a differentially corrected global positioning system (GPS), laser rangefinder, and electronic compass.

The Tahoe study area (39.62°N, 120.78°W) is within the Yuba district of Tahoe National Forest in northern California. Elevations in the study area range from approximately 1000 to 2000 m above sea level. The main forest species in this region are coniferous, including white fir (*Abies concolor*), red fir (*Abies magnifica*), incense cedar (*Calocedrus decurrens*), Jeffrey pine (*Pinus jeffreyi*), ponderosa pine (*Pinus ponderosa*), sugar pine (*Pinus lambertiana*), western white pine (*Pinus monticola*), and Douglas fir (*Pseudotsuga menziesii*). There are also several deciduous species such as bigleaf maple (*Acer macrophyllum*), California black oak (*Quercus kelloggii*), and canyon live oak (*Quercus chrysolepis*); although these account for a small fraction of stems and biomass in the forest (Waring et al., 2006). DRL at this site was used to calibrate GLAS estimates of height. Field data from Tahoe were used to compare Lorey's and crown-area-weighted height and to calibrate GLAS estimates of height. For the comparison of Lorey's and crown-area-weighted height, plots at these sites conformed to the layout and sampling design of the US Department of Agriculture (USDA) Forest Service Forest Inventory and Analysis Program (see Sherrill et al., 2008 for details), and data at the subplot level were used for these analyses.

The San Bernardino site (34.19°N, 117.15°W) in southern California is on a generally south facing slope with elevations ranging from 1300 to 1700 m. This site is occupied by the shrub and tree species common in the very dry chaparral ecosystems of this region, including chamise (*Adenostoma fasciculatum*), deer brush (*Ceanothus integerimus*), various manzanita species (*Arctostaphylos* spp.), canyon live oak (*Quercus chrysolepis*), California scrub oak (*Quercus dumosa*), Coulter pine (*Pinus coulteri*), ponderosa pine (*Pinus ponderosa*), and white fir (*Abies concolor*). DRL from San Bernardino was used to calibrate GLAS estimates of height.

Three sites in Colorado and southern Wyoming were used to compare Lorey's and crown-area-weighted height. The Niwot Ridge Long Term Ecological Research site is located approximately 35 km west of Boulder, Colorado, on the drier eastern side of the continental divide, with plot locations occurring at elevations between 3035 and 3115 m. The Fraser Experimental Forest (FEF) is part of the Rocky Mountain Research Station, managed by the USDA Forest Service, and is located approximately 80 km west of Denver, Colorado, and 30 km southwest of the Niwot site on the wetter western side of the continental divide, with plots at elevations between 3030 and 3230 m. The Glacier Lakes Ecosystem Experiments site (Glees) is located 60 km west of Laramie, Wyoming, in the Medicine Bow Mountains (approximately 160 km north-northwest of the Niwot and Fraser sites), with plots at elevations between 3175 and 3220 m. All three study sites are dominated by subalpine forest types, which include Engelmann spruce (*Picea engelmanni*), subalpine fir (*Abies lasiocarpa*), lodgepole pine (*Pinus contorta*), limber pine (*Pinus flexilis*), and aspen (*Populus tremuloides*) tree species. Plots at these sites conformed to the layout and sampling design of the USDA Forest Service Forest Inventory and Analysis Program (see Sherrill et al., 2008 for details), and data at the subplot level were used for these analyses. These data and coincident DRL were used to compare the Lorey's and crown-area-weighted height.

Airborne discrete return lidar data

Lidar data covering the test sites were collected between 2004 and 2006 using a variety of sensors (**Table 2**). Only high point density (for six sites > 2 shots/m², for one site > 1.5 shots/m²) lidar data collected during ICESat operations were used. In total, 421 subset plots (with co-located GLAS observations and airborne lidar datasets) were located at four sites in western North America from California to Alaska. Data were obtained in the form of point cloud coordinates (x, y, z) with intensity values. In this work, the digital terrain model (DTM) used to calculate height from elevation was generated using various published lidar point data filters. A progressive morphological filter (Chen, 2007) was used for Tahoe, Niwot, Fraser, and Glees data. For the Mission Creek and Bonanza Creek lidar datasets, ground points were filtered by the vendor using the Terrascan software system, and a DTM was provided as a deliverable. For the San Bernardino lidar data, the ground points were filtered using an algorithm described in Andersen et al. (2006). Estimates of height for each lidar point were calculated as the difference between the elevation of the point and the elevation of the DTM at that location.

Indices of stand heights

We apply a mean stand height weighting scheme, namely the crown-area-weighted height, not used frequently in the ecological literature but ideally suited for lidar. This index is conceptually and, as shown here, empirically similar to the Lorey's height (Avery and Burkhart, 2002) already in common use in forestry and demonstrated to be highly correlated with

field estimates of both height and aboveground biomass (Lefsky et al., 2005). Lorey's height is defined as

$$\text{Lorey's height} = \frac{\sum G_i H_i}{\sum G_i} \quad (1)$$

where G_i is the basal area of stem i , and H_i is the height of stem i . Similarly, we define crown-area-weighted height as

$$\text{crown-area-weighted height} = \frac{\sum C_i H_i}{\sum C_i} \quad (2)$$

where C_i is the projected crown area of stem i . Lorey's height and crown-area-weighted height are conceptually related by their common use of tree height weighted by each tree contribution to the total forest structure. The degree of consistency in the two indices is determined by the consistency of the ratio between crown area and basal area of individual stems within a single plot. When the ratio varies, the weights derived from crown diameter will differ from those based on tree basal area, although the actual value of the ratio does not influence the calculations.

Tree crown delineation

Crown-area-weighted height could be estimated using conventional field methods, but it is the ability to estimate it using discrete return lidar that is of interest here. To address the estimation of forest height from the global database of GLAS waveforms, we require a crown delineation technique that will yield accurate estimates of crown-area-weighted height in many types of forests. As a first step in this direction, we developed a crown delineation algorithm to identify dominant and codominant tree crowns from DRL data using a combination of local-maximum, region-growing, and curve-fitting methods. The tree crown delineation method is summarized in the following steps.

Canopy height model generation

The tree CHM depicts the uppermost elevations of the forest, including the top surface of the canopy or the ground surface where there are no trees; these elevations were normalized to height above terrain elevation using a "bare-earth surface" DTM. The CHM was created by interpolating the normalized height of lidar points to a regular grid with a spatial resolution of 0.5 m using the triangulated irregular network (TIN) method. Lidar points used for creating the CHM included only the highest points in 0.5 m × 0.5 m cells to allow for an accurate characterization of the top canopy surface. The interpolated CHM has some holes because of missing data; a low-pass Gaussian filter was used to remove these effects.

Tree-top detection

The local-maxima method is used to detect tree tops. The main problem with this method is the high likelihood of

commission error (Zhao and Popescu, 2007). Variably sized smoothing windows (Solberg et al., 2006) or a locally adaptive search window size (Popescu et al., 2003) is often used to minimize this phenomena. Although these techniques may improve accuracy, they require supervision or local prior knowledge, which prevents their practical use over large areas or areas where no ground data are available. A 3 × 3 window was used to detect local maxima in this study, although it will result in some commission errors. A larger window size can decrease commission errors but will increase omission errors.

In our work, highly accurate representation of the scene can be sacrificed if accurate estimates of the crown-area-weighted height can be preserved. For instance, if adjacent trees of similar size cannot be distinguished but the total area of their crowns and their average height are correctly estimated, the influence of this error on crown-area-weighted height might be minor. On the other hand, if a tree has a multi-peaked crown, commission error will result. Given that the sum of these over-segmented tree crowns area is close to the real crown area, it will still have a slight effect on crown-area-weighted height. Commission errors can be addressed further by analysis of overlapping crowns.

Identification of dominant and codominant trees

Previous studies have shown that only the dominant tree layer is detected accurately in crown delineations based on CHM surfaces. Since the upper canopy surface consists primarily of the tallest dominant and codominant trees, the suppressed and subdominant trees are rarely identified (Popescu et al., 2003; Solberg et al., 2006). However, the dominant and codominant trees have the greatest contribution to the GLAS waveform and the overall stand height and aboveground biomass of an area, and therefore we focus on estimates for these trees. Adapting a common field measurement definition, we defined dominant and codominant trees as those taller than the 40th percentile height of the tallest trees in four quadrants within a 35 m radius (**Figure 1a**). This definition can be implemented in a uniform manner using the local maxima identified in that previous step. The definition of dominant and codominant stems is used to allow direct comparison with field data for only those stems that are the main contributors to the crown-area-weighted height.

Region growth to extract height profiles

Field measurements of crown width are generally calculated as the average of four radii measured with a tape from the bole of a tree towards each cardinal direction. When derived from a canopy height model, this measurement is made using region growing (Culvenor, 2002). The pixels that are neighbors of a local-maxima point are evaluated, and those that satisfy a series of criteria are added to the region; the resulting set of pixels is then compared to their neighbors. Each region continues to grow until it either runs out of acceptable pixels or reaches a critical maximum size or shape limit (Erikson, 2003). In this work, we started from each local-maxima point and extracted height profiles in eight directions (**Figure 1b**). In each

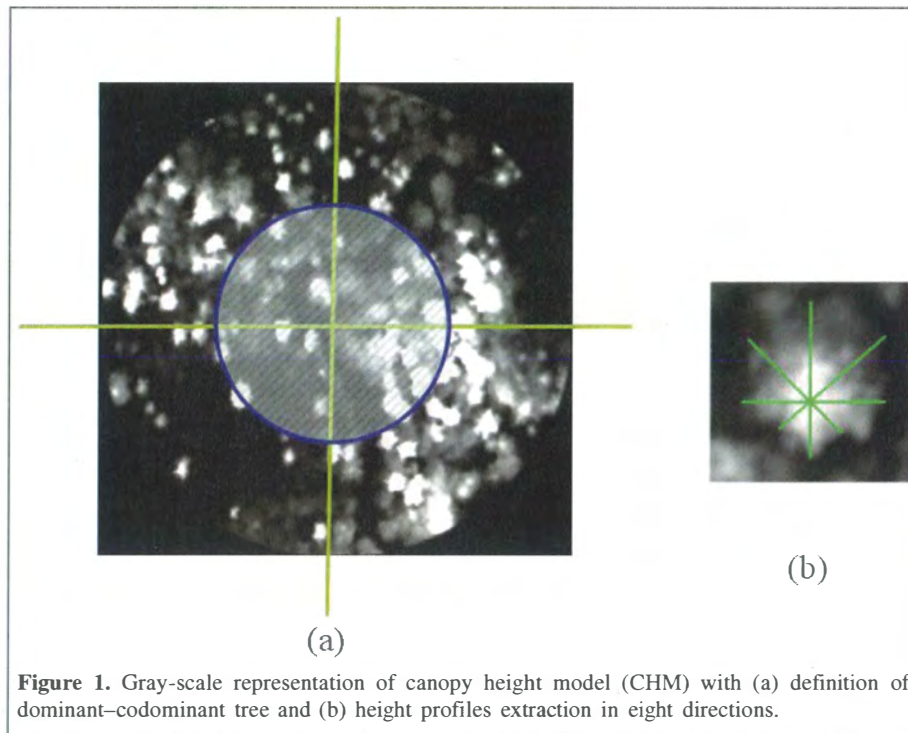


Figure 1. Gray-scale representation of canopy height model (CHM) with (a) definition of dominant-codominant tree and (b) height profiles extraction in eight directions.

direction, new pixel values were added to the profile if the new pixel is at a lower height than the prior pixel and above an estimate of height of the crown edge (in this study, one tenth of the tree height). A similar scheme was used by Pouliot et al. (2005) for aerial photographs.

Estimates of crown diameter

A fourth-order polynomial was fit to each height profile (Pouliot et al., 2005; Popescu et al., 2003) using the interactive data language (IDL) implementation of the MPFIT package, a robust least-squares curve-fitting package based on the Levenberg-Marquardt algorithm (cow.physics.wisc.edu/~craig/idl/fitting.html). A fourth-order polynomial can have a concave shape along the crown profile of a single tree. Extreme points can be identified using the first derivative of the fit function; those extreme points with a negative sign in the second derivative are identified as the locations of local minima, i.e., crown edge points (see Popescu et al., 2003 for details). The crown diameter along that direction is calculated using the distance between two local-minimum locations. As some fitting processes could not get convergent results, the crown diameter for a specific tree is the average of all the diameters that converged. Maximum and minimum crown diameters were also determined. We define the “crown inner radius” as the minimum crown radius minus the CHM spatial resolution, which delineates the region with a high likelihood of being the true tree crown extent. The maximum height value within the circle of the crown inner radius from the unfiltered CHM is used as the tree height. In a few cases, no profiles from an

individual tree were convergent, and the CHM value of tree-top location is set as tree height, and crown diameter is set as the larger of either (i) one tenth of tree height or (ii) two times the CHM spatial resolution.

Removal of crown overlaps

As multiple local maxima could be associated with a single tree, some commission errors may occur after the previous delineation steps. To address this problem, if one tree top is located in another crown inner radius circle, the shorter tree top will be deleted and the higher tree top will be kept. The larger crown parameter will be assigned to the tree that was kept, and this refinement is continued until the number of tree tops does not change. A file is generated that contains each individual tree’s information, including tree location coordinates, crown width, and height.

Evaluation of crown delineation

We evaluated the crown delineation algorithm in two ways. First, we compared the location of field-identified and lidar-delineated trees for 12 stem-mapped plots at the Mission Creek site. If a codominant and a dominant field-identified tree fell within the estimated (lidar-based) crown radius, it was considered a match. Due to a combination of GPS, rangefinder, and compass errors, there is a 1 m uncertainty in the coordinates of individual trees in the stem map. Taken together with the horizontal uncertainty of the lidar positions, which may be as large as 50 cm even in data with acceptable registration errors,

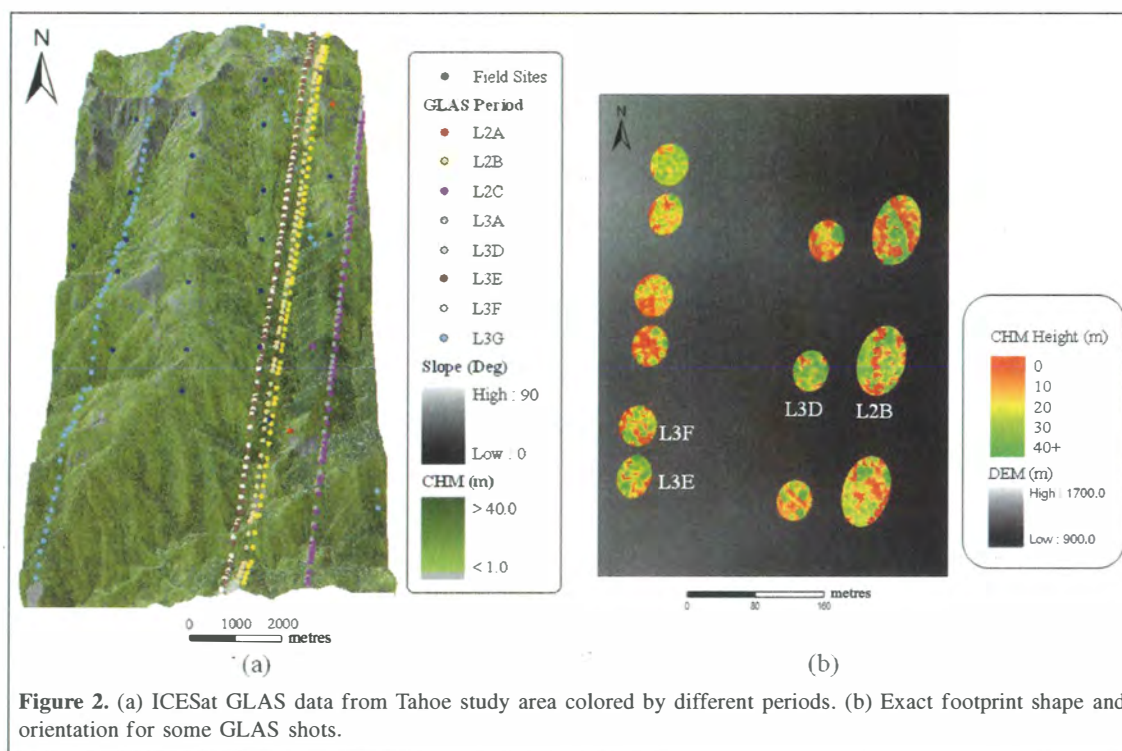


Figure 2. (a) ICESat GLAS data from Tahoe study area colored by different periods. (b) Exact footprint shape and orientation for some GLAS shots.

we allowed a tree to be considered a match if it was within a 1.5 m buffer of its apparent location in the lidar data.

We then compared field estimates of Lorey's height from 242 plots at five sites (Fraser (48), Glees (48), Mission Creek (66), Niwot (48), and Tahoe (32)) to estimates of crown-area-weighted height derived from the crown delineation algorithm applied to our airborne lidar data. Quality of fit was evaluated by r^2 and root mean square error (RMSE) statistics. Although further validation of the crown delineation technique will be required for other types of forests, these two analyses provide a high level of confidence for the purpose of estimating a plot-level crown-area-weighted height in these forests. Further validation will be required before using this technique for the purpose of identifying individual tree location and crown metrics.

ICESat GLAS data

We evaluated the ability of our estimates of crown-area-weighted height to serve as training data for height estimates from GLAS waveforms. There were 11 GLAS observation periods between 2003 and 2006; data from seven of these periods were represented at the four sites used for the GLAS analysis (Bonanza Creek, Mission Creek, San Bernardino, and Tahoe). Data from the other sites were not available at the time these analyses were performed. **Figure 2** shows GLAS waveforms from the Tahoe study area colored by different periods. GLAS waveforms from observation periods L2A, L2C, L3A, and L3G were removed due to low signal-to-noise ratios for the observations at our sites, as were any other waveforms with a maximum waveform power less than 80

unscaled waveform units. Low signal-to-noise ratios reflect both a long-term trend of declining power for each laser and specific environmental conditions at the time of data acquisition (e.g., atmospheric transmittance at 1064 nm). GLAS data from the ICESat vegetation product (IVP-<http://ceal.cnr.colostate.edu>) were used for this project.

Three indices are calculated from the GLAS waveform (**Figure 3**) to estimate forest canopy height. Waveform extent is defined as the vertical distance between the first and last elevations at which the waveform energy exceeds a threshold level. In this work, the threshold was determined using ICESat data product estimates of the mean and standard deviation of background noise (ICESat product variables $D_4NSBGMEAN$ and $D_4NSBGSDEV$). Removal of the effects of terrain slope and canopy height variability relies on two other indices of waveform structure. The trailing-edge extent is calculated from the waveform as the absolute difference between the elevation of the signal end and the elevation at which the signal strength of the trailing edge is half of the maximum signal above the background noise value. Similarly, the leading-edge extent is determined as the absolute difference between the elevation of the signal start and the elevation at which the signal strength of the leading edge is half of the maximum signal above the background noise value. At the leading edge of the waveform, the "signal start" threshold crossing indicates the elevation of the uppermost foliage and (or) branches that were detected, and the trailing-edge threshold crossing indicates the elevation of the lowest illuminated surface, or the "signal end." Where sufficient laser energy is reflected from the ground, signal end

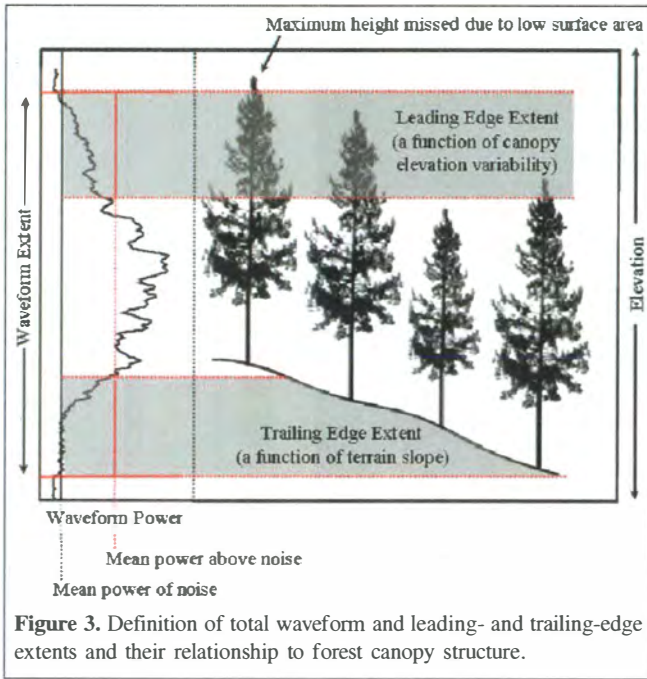


Figure 3. Definition of total waveform and leading- and trailing-edge extents and their relationship to forest canopy structure.

crossing represents the lowest detected ground surface. Details of GLAS data processing can be found in Lefsky et al. (2007).

GLAS records the laser energy returned from an ellipsoidal footprint. The nominal footprint diameter is 70 m, but its size and ellipticity varied through the course of the mission. The computed sizes determined from instrumentation on board the spacecraft are closer to about 110, 90, and 55 m for lasers 1, 2, and 3, respectively (nsidc.org/data/icesat/glas_laser_ops_attrib.pdf).

Comparison of ICESat and DRL datasets

To compare the ICESat data with the results of the crown delineation, discrete return lidar data within 100 m from the center of each waveform footprint were extracted. Individual crowns were delineated from the data, and their position, area, and height of the crowns were recorded. The azimuth angle, major axis radius, and eccentricity fields in the ICESat-GLAS GLA05 product were used to extract all delineated crowns from within the exact shape of the ICESat GLAS footprint:

$$\begin{cases} \text{ellipse_}a = [i_tpmajoraxis \times \text{sqrt}(1 - i_tpeccentricity^2)] / 2 \\ \text{ellipse_}b = i_tpmajoraxis / 2 \\ \text{azimuth} = i_beam_azimuth \end{cases} \quad (3)$$

where ellipse_a and ellipse_b are the radius of the minor and major axes, respectively, of the GLAS footprint; i_beam_azimuth (i.e., the azimuth) is the direction clockwise from north of the laser beam vector as seen by an observer at the laser ground spot viewing toward the spacecraft (i.e., the vector from the ground to the spacecraft); and i_tpmajoraxis and i_tpeccentricity are the major axis and eccentricity, respectively, of the transmit pulse measured by the laser

profiling array (LPA) (wffglas.wff.nasa.gov/v50_products/). Individual tree data within the footprint were extracted using the criterion expressed in the following equation:

$$\frac{[x_i \cos(\text{azimuth}) - y_i \sin(\text{azimuth})]^2}{\text{ellipse_}a^2} + \frac{[x_i \sin(\text{azimuth}) + y_i \cos(\text{azimuth})]^2}{\text{ellipse_}b^2} \leq 1 \quad (4)$$

where x_i and y_i are the coordinates of stem i. The crown-area-weighted mean height was then calculated from the individual crowns using Equation (2).

Estimates of crown-area-weighted height from GLAS

In earlier work (Lefsky et al., 2007), stepwise multiple regressions were used to find a relationship between waveform indices and tree heights. In that work, we used multiple transformations of the three basic waveform indices, which resulted in the following equations:

trailing-edge correction factor

$$\begin{aligned} &= 3.4\sqrt{\text{trail}} + 0.92 \times \text{trail} - 88.5 \frac{\text{trail}}{\text{extent}} + 2049.5 \\ &+ \frac{\text{trail}}{\text{extent}^2} - 14171.4 \frac{\text{trail}}{\text{extent}^3} \end{aligned} \quad (5)$$

and

$$\text{leading-edge correction factor} = 0.72 \times \text{lead} - 21.8 \frac{\text{lead}}{\text{extent}} \quad (6)$$

In the second step of the analysis, the multiple transformations of the trailing-edge indices are summarized as a trailing-edge correction factor, and a similar leading-edge correction factor is defined as well, which results in the following equation:

height = width

$$\begin{aligned} &- [8.96 + (1.52 \times \text{leading-edge extent factor}) \\ &+ (1.14 \times \text{trailing-edge extent factor})] \end{aligned} \quad (7)$$

This equation provided an excellent fit to the data (83% of variance, and RMSE = 4.9 m), and the coefficients were highly interpretable in terms of ancillary data we had for the 197 plots in that dataset. However, when applied to a larger dataset of GLAS waveforms, the numerous ratios led to situations in which unreasonable estimates were made, especially when waveform extent was small. To test the effect of a simpler equation on the quality of the estimates, we used MPFIT to relate the crown-area-weighted heights to the three GLAS height indices using the following equation:

$$b_0 \times \text{waveform_extent} - [b_1 (\text{lead} + \text{trail})]^{b_2} \quad (8)$$

Regression methods

In evaluating our regressions, we report r^2 or R^2 for statistically significant (at $p < 0.05$) regressions, the RMSE, and equation intercept and coefficients. For predicted versus observed comparisons, we report two estimates of the intercept and slope, one derived from ordinary least squares (OLS) regression and the other from reduced major axis (RMA) regression. RMA minimizes the sum of squared orthogonal distances from measurement points to the model function. Mathematical similarities in the formulations of OLS and RMA regression models mean that the model intercepts are all equivalent, as are the coefficients of determination. What differs among these models are the RMSEs and the slopes of the relationships. When both the dependent and independent variables are estimates with associated error, slope coefficients derived using least ordinary squares regression will be biased (Sokal and Rohlf, 1981). Although the slope and intercept results from RMA better represent the relationship between predicted and observed data, we report those from OLS for reference because they are more commonly used.

Results

Tree crown delineation

Figure 4 illustrates the performance of the crown delineation method for one of 12 stem maps at the Mission Creek study area. Most field-measured dominant and codominant trees were located within or near lidar-detected trees. The largest differences were located at the plot boundaries. As is indicated by the blue circles in **Figure 4**, more trees were detected with the local-maximum method; these are commission errors. After the removal of crown overlaps, these commission errors were corrected in most cases.

The 12 Mission Creek plots included 40 dominant trees and 135 codominant trees. Of these trees, 34 dominant trees and 106 codominant trees were directly matched to crowns delineated from the DRL. The r^2 for individual tree height was 0.88, with an RMSE of 2.05 m; the slope is close to 1 (1.004), and the intercept is close to 0 (0.5948 m) (all p values $\ll 0.01$). Our crown delineation method resulted in individual tree height estimates comparable in accuracy with those from the previous studies as listed in **Table 1**.

Figure 5 shows the regression between Lorey's height from field measurements and crown height from lidar crown delineation for 242 plots in the Fraser, Glees, Mission Creek, Niwot, and Tahoe study areas. Using OLS regression, the r^2 for individual tree height is 0.76 and the RMSE is 3.8 m, with a slope of 0.86 and an intercept of 2.3 m. The more accurate slope and intercept estimates derived from RMA are 0.98 and -0.8 m, respectively.

IVP evaluation using crown-area-weighted mean height

We generated crown-area-weighted mean height for 421 plots located at four sites in western North America from

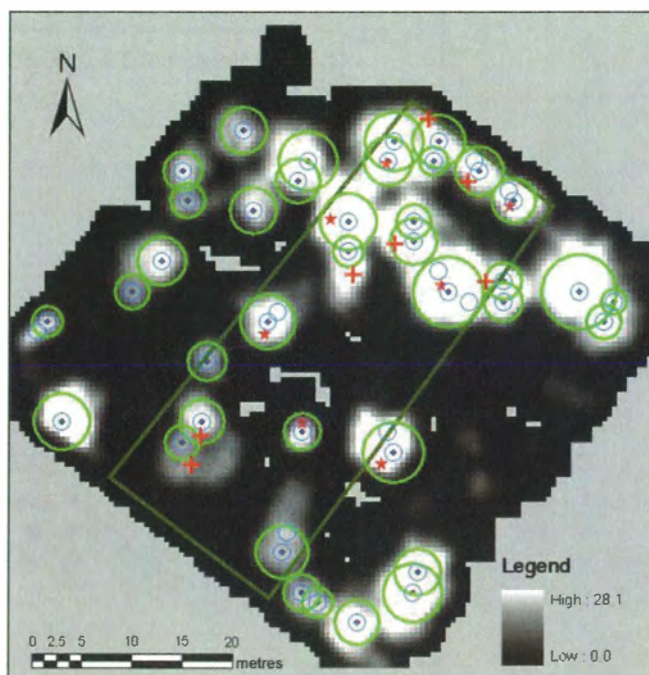


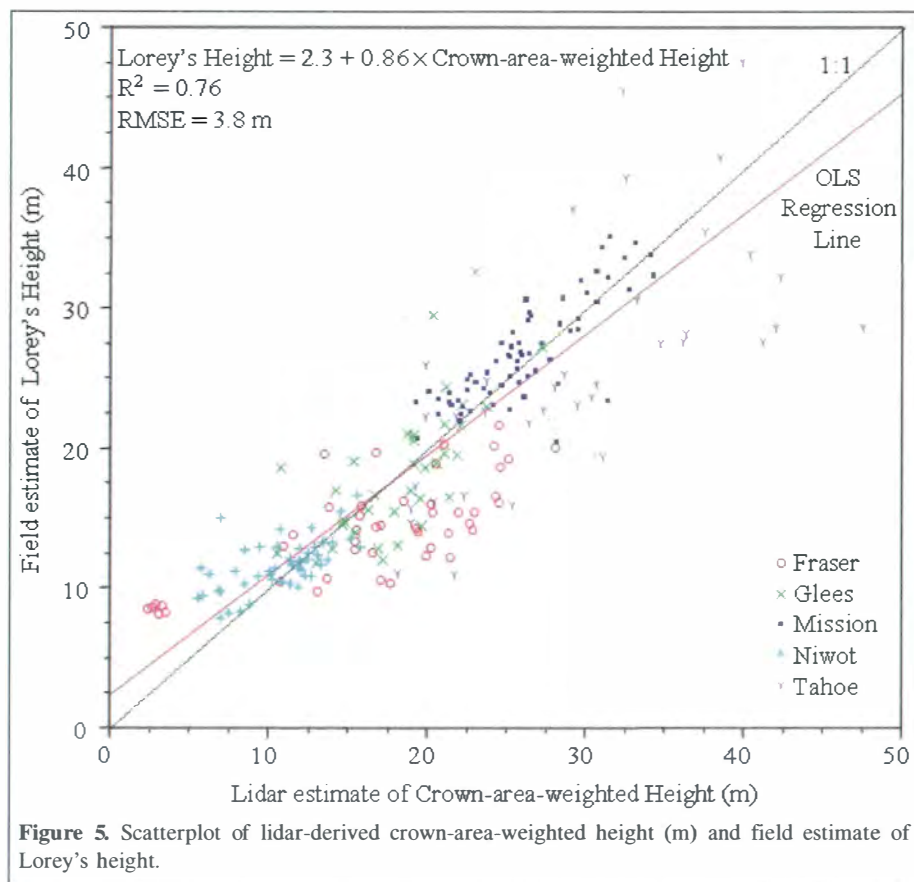
Figure 4. Illustration of the performance of the crown delineation algorithm. Blue circles are lidar-detected tree locations before refinement; blue dots are lidar-detected tree locations after refinement; red stars and plus symbols are field-measured dominant and codominant tree locations, respectively; light green circles are estimated crown radius; and the dark green rectangle is the field plot boundary.

California to Alaska. Parameterizing Equation (8) with the plot dataset from Bonanza Creek, Mission Creek, San Bernardino, and Tahoe resulted in the following equation:

$$\text{crown-area-weighted height} = 0.556 \times \text{waveform_extent} - [18.7(\text{lead} + \text{trail})]^{-0.406} \quad (9)$$

This equation resulted in consistent relationships between the crown-area-weighted height from airborne DRL data and forest height estimated from GLAS (**Figure 6**). The r^2 is 0.69 and RMSE is 6.2 m, with a slope of 0.98 and an intercept of 0.62 m. This result is similar to those obtained from regression analysis of GLAS waveforms with field estimates of forest height (Lefsky et al., 2005) or a combination of field and lidar estimates of height (Lefsky et al., 2007).

When we use the crown height from the DRL data to evaluate the previously published equation (Lefsky et al., 2007), it shows a linear relationship with an r^2 of 0.54 and an RMSE of 7.4 m (**Figure 7**). Using OLS regression, the slope is 0.84 and the intercept is 3.9 m, whereas with RMA the slope is 1.14 and the intercept is 0.29 m. It should be noted that Lefsky et al. (2007) dealt with the prediction of the mean height of dominant and codominant stems, an index similar to but distinct from the crown-area-weighted height used in this paper.



Discussion

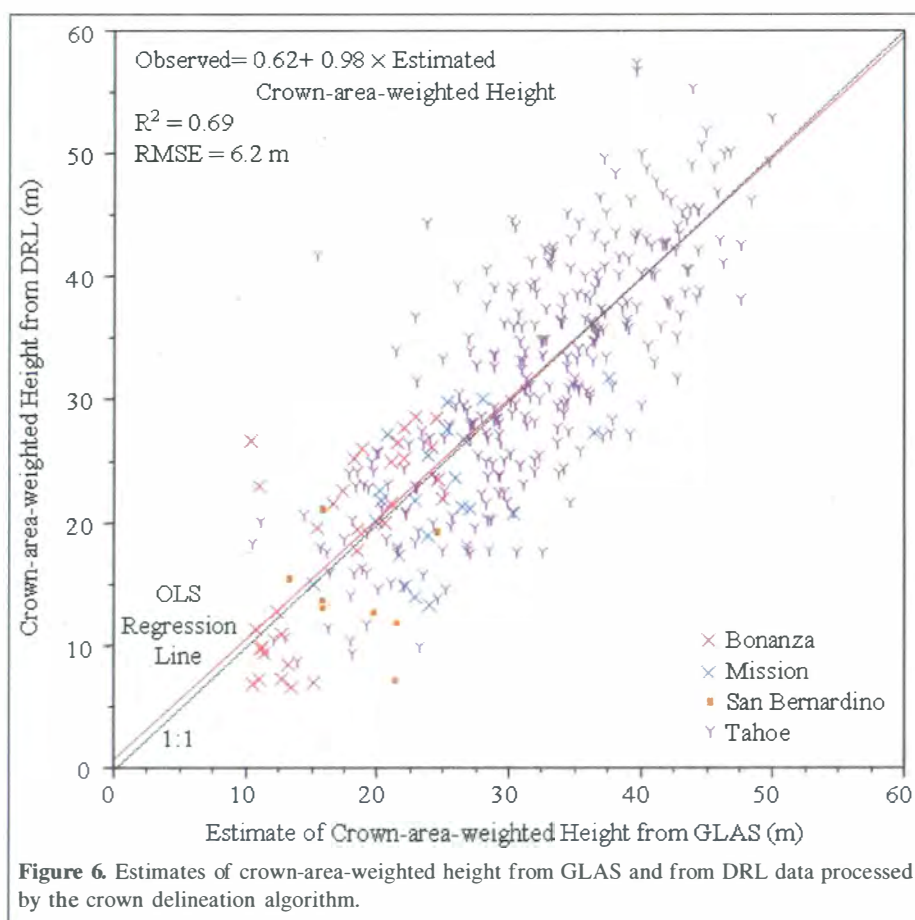
The crown-area-weighted mean height was used in this study because it is easily applied to field, discrete-return lidar, and model results and is conceptually and quantitatively similar to Lorey's height, which is widely used in forestry. As a consequence, relationships developed from field inventory (such as between Lorey's height and aboveground biomass) could be calibrated and applied to remotely sensed estimates of crown-area-weighted height. Previous studies have tried to estimate the maximum height or the mean height of dominant and codominant stems. Maximum height fulfills the need for a height metric that can be derived from forest inventory data and (with sufficiently dense observations) directly observed in DRL. However, maximum height is unsuitable for large-footprint lidar, as their waveforms are often insensitive to the very tops of conical crowns because the small surface area of the uppermost branches and leaves does not reflect enough energy to reliably rise above the background noise of the waveform. The definition of dominant and codominant stems varies among sites and is difficult to apply to some datasets. We use a straightforward definition of dominant and codominant stems in this work to aid in comparison with field estimates, but that definition is unlikely to exclude the largest trees, and the crown-area-weighting process will minimize the influence of

any smaller stems that are incorrectly included as dominant or codominant stems.

In performing the crown delineations, we defined dominant and codominant trees as those taller than the 40th percentile height of the tallest trees in four quadrants within a 35 m radius. In work leading up to this study, various height thresholds were tested for defining dominant–codominant trees. When 30th, 40th, and 50th percentile heights are used, the detected trees are different, but they did not translate into obvious differences in crown-area-weighted height at the GLAS footprint level. Since the upper canopy surface consists primarily of the tallest dominant and codominant trees, the suppressed and subdominant trees are rarely identified and they usually have low height and small crowns.

The degree of agreement between Lorey's and crown-area-weighted height is a function of the consistency of the ratio of stem to crown diameter within a single stand. That consistency was noted by early workers in forestry (Duhaufour, 1903) and remote sensing (Zieger, 1928). Spurr (1948) reviews early studies of six conifer species and five deciduous species, all of commercial interest, and indicates a reliable relationship in all cases, although he notes the effect of stem density.

Hemerya et al. (2005) review 11 commercial species and indicate that some species have higher crown to stem diameter ratios when under 20 cm dbh. The existence of this sort of bias may not conflict with the use of crown-area-weighted height as



a proxy for Lorey's height. Such stems might occur in low-stature stands, which tend to have a large number of equal-sized stems (in which case all stems will have similar ratios) or in stands with larger trees (in which case they may not make an important contribution to total crown area).

Tree crown delineation

The method proposed in this paper assumes that all local maxima are the tops of individual trees, which will cause some commission errors for those trees with multiple tops or large extruding branches. The "removal of crown overlap" step can reduce this error only if a false tree top has a small radius and is not far from the real tree top. In some deciduous and older coniferous forests, one tree might have several large sparse branches that could appear to be several separated tree crowns, which might cause problems for our current method. However, even in this case, the sum of the areas of these over-segmented tree crowns will be close to the real crown area. Therefore, the commission error in crown delineation has few effects on crown height if all of these peaks have similar heights.

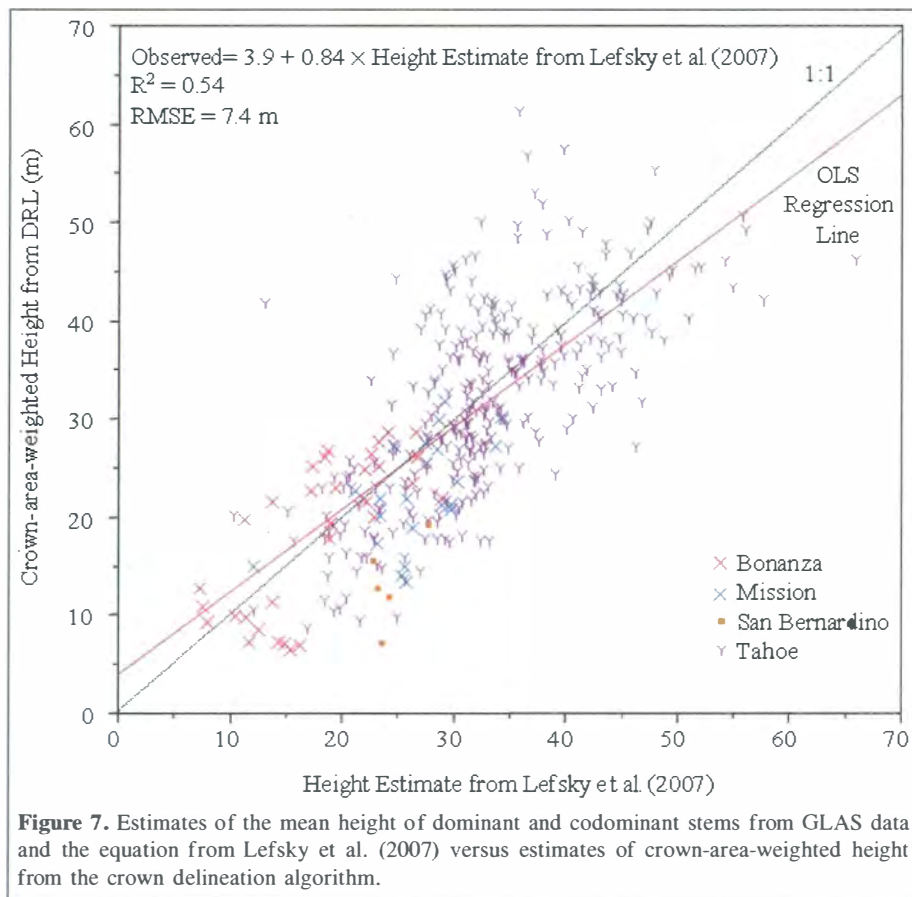
The region-growing method used to extract the height profile around tree tops can also be hindered in complex forest environments where crown apices are difficult to identify or

multiple crown peaks are commonplace. Koch et al. (2006) also pointed out a similar problem in their pouring algorithm. In addition, a circular crown shape was used to calculate crown area. In reality, some crowns tend to be asymmetrical with irregular edges. Other shapes will be tested with crown radii estimated in eight directions for improving crown area calculation in the next step of this work.

Previous results suggest that lidar techniques tend to underestimate tree height due to the probability of missing tree tops even with high-density laser data (Andersen et al., 2006; Popescu et al., 2003; Yu et al., 2004; Solberg et al., 2006; Chen et al., 2006). Some correction methods have been used, such as CHM lifting (37 cm was used in Solberg et al., 2006). However, a lidar DTM under a conifer forest canopy may have an error at least as large as 0.31 ± 0.29 m (mean \pm standard deviation) for dense canopy (Reutebuch et al., 2003). We concluded that the uncertainty of the underlying elevation of the CHM was large enough that no correction to the CHM was warranted for our purposes.

Height estimates from GLAS

In the context of airborne DRL-based forest inventory applications, an RMSE of 6.2 m would be an unsatisfactory



result. However, given the limitations of the GLAS sensor, these results may represent the best that can be achieved for forests with substantial terrain slope (e.g., $>10^\circ$ slope). As related in Lefsky et al. (2007), model-based analysis of this problem indicates that 5 m RMSE represents the best accuracy we can expect without ancillary data. Although individual height estimates from GLAS are uncertain, they are being used in the context of developing estimates over large scales (tens to hundreds of square kilometres). In that type of analysis, the availability of hundreds of millions of observations makes possible the reduction of uncertainty by the averaging of observations. For instance, 7 km of GLAS transect (with observations every 170 m) provides enough observations to reduce measurement error from 6 m to 1 m RMSE.

Models of lidar remote sensing

A reoccurring theme in remote sensing is the use of coarse spatial resolution data to characterize objects that are smaller than the resolution of those measurements, i.e., the discrete L-resolution model approach of Strahler et al. (1986). This is the case for the type of spaceborne lidar systems currently operating (GLAS) or envisioned (Veg3d type sensors; www.veg3dbiomass.org), where the spatial scale of measurements is 25–70 m, or two to twenty times the width of a

mature tree crown. In such cases the size and spatial distribution of objects within the footprint are unknown and a unique inversion of the scene may not be possible or may only be possible by assuming (implicitly or explicitly) a statistical distribution of object size and spatial location in three dimensions.

When working with discrete return lidar, the data processing model typically corresponds to the continuous or discrete H-resolution model (Strahler et al., 1986). Methods that deal with the horizontal and vertical distribution of the canopy as a whole are continuous models: they are used to estimate bulk properties of either canopy cover (e.g., the mean height or projected area of foliage and other canopy surfaces) or of energy returned from the canopy (e.g., the height of median energy or HOME). Although these properties of the canopy are intrinsically interesting, they are not directly related to traditional measurements either of individual trees (e.g., individual tree height or crown depth) or of tree stands (e.g., the height of dominant and codominant trees), but they are highly correlated with and can be calibrated to coincident measurements of that type. Analyses in which the scale of observations is much smaller than the scale of scene objects can also use discrete H-resolution models. When this approach is applied to applications in forestry or forest ecology, the H-resolution model can typically take the form of individual tree

crown delineation or segmentation. In these analyses, high-density lidar measurements are collected and individual tree crowns are identified in the resulting point cloud. The advantage of such an approach is that it results in estimates of variables that are conceptually (and often empirically) related to traditionally collected tree level measurements. These measurements can then be summarized to estimate the measurements traditionally made at the plot or stand level. For instance, the height, crown width, and crown depth of individual trees can be estimated directly using this approach, the crowns can be classified into dominant and codominant stems, and their mean heights can be calculated.

Advances in the solution of discrete L-resolution problems often rely on ancillary remotely sensed data that complement the coarse resolution of the primary (L-resolution) data. Advantages of this approach include those making remotely sensed data useful in the first place: accuracy, precision, correspondence to existing measurements, rapid and low-cost data collection, and flexible data processing. However, for the L-resolution class of problem the primary advantage is the ability to explicitly characterize the size and spatial distribution of objects in a manner that is directly comparable with the coarser dataset. Comparison between datasets at different scales is not always so direct. For instance, the type of data collected in field investigations of forests typically includes the diameter of tree stems, tree species, and possibly overall tree height. Crown geometry data or geographic position are rarely collected, and then typically only for a subset of trees. Although these measurements can be related to remotely sensed data statistically, they are fundamentally different in type from the type of observations made by imaging or lidar sensors. For imaging sensors, the types of surface cover and their spectral qualities are of most importance. For lidar remote sensing of forests, crown size, three-dimensional shape, and three-dimensional location are the most critical measurements needed to relate small-scale objects to large-scale observations. Using high-density collections of discrete return lidar data and the crown segmentation approach, we can quickly generate datasets that allow us to quickly and reliably parameterize models of forest height using GLAS waveforms and discrete return lidar remote sensing.

Conclusion

Dominant and codominant tree crowns were delineated from discrete return light detection and ranging (DRL) data in several different coniferous forest types in western North America. Of the dominant and codominant stems in the field data, 80% were identified; the r^2 for these individual tree heights was 0.88 (root mean square error (RMSE) of 2.05 m). Lorey's height from field measurement shows a good linear relationship with crown-area-weighted mean height from lidar data ($r^2 = 0.76$, RMSE = 3.8 m, intercept = 0.8 m, and slope = 0.98). Further analysis will be required to determine the utility of this particular crown delineation technique for deciduous forests.

The crown-area-weighted mean height estimates from the DRL data were successfully used for parameterizing an equation to estimate height from Geoscience Laser Altimeter System (GLAS) waveform indices and for Ice, Cloud, and Land Elevation Satellite (ICESat) GLAS vegetation product validation ($n = 421$, $r^2 = 0.69$, RMSE = 6.2 m). More DRL datasets have been collected for GLAS forest height validation and will form the basis of canopy height modeling and validation globally.

Acknowledgments

This research is supported by the NASA grants NNX06AH36G, NNG04GO73G, and NNG06GE11A. The authors would like to thank the Wenatchee National Forest, Joint Fire Science Program, USDA Forest Service Pacific Northwest Research Station, and the University of Washington Precision Forestry Cooperative for providing field and lidar data for the Mission Creek and San Bernardino sites, and the University of Alaska-Fairbanks for providing lidar data for the Bonanza Creek site. Y. Pang would like to thank the support from the National 863 project of China (No. 2007AA12Z173).

References

- Andersen, H.-E., Reutebuch, S.E., and Schreuder, G.F. 2001. Automated individual tree measurement through morphological analysis of a LIDAR-based canopy surface model. In *Proceedings of the 1st International Precision Forestry Symposium*, 17–20 June 2001, Seattle, Wash. College of Forest Resources, University of Washington. Seattle, Wash. pp. 11–22.
- Andersen, H.-E., Reutebuch, S.E., and McGaughey, R.J. 2006. A rigorous assessment of tree height measurements obtained using airborne lidar and conventional field methods. *Canadian Journal of Remote Sensing*, Vol. 32, No. 5, pp. 355–366.
- Avery, T.E., and Burkhart, H.H. 2002. *Forest measurements*. 5th ed. McGraw Hill. New York. 456 pp.
- Brandtberg, T., Warner, T.A., Landenberger, R.E., and McGraw, J.B. 2003. Detection and analysis of individual leaf-off tree crowns in small footprint, high sampling density lidar data from the eastern deciduous forest in North America. *Remote Sensing of Environment*, Vol. 85, No. 3, pp. 290–303.
- Chen, Q. 2007. Airborne lidar data processing and information extraction. *Photogrammetric Engineering & Remote Sensing*, Vol. 73, No. 2, pp. 109–112.
- Chen, Q., Baldocchi, D., Gong, P., and Kelly, M. 2006. Isolating individual trees in a savanna woodland using small footprint lidar data. *Photogrammetric Engineering & Remote Sensing*, Vol. 72, No. 8, pp. 923–932.
- Culvenor, D.S. 2002. TIDA: an algorithm for the delineation of tree crowns in high spatial resolution remotely sensed imagery. *Computers & Geosciences*, Vol. 28, No. 1, pp. 33–44.
- Duchaufour, A. 1903. L'aménagement de la forêt de Compiègne. *Revue des Eaux et Forêts*, Vol. 42, pp. 65–78.
- Erikson, M. 2003. Segmentation of individual tree crowns in colour aerial photographs using region growing supported by fuzzy rules. *Canadian Journal of Forest Research*, Vol. 33, No. 8, pp. 1557–1563.

- Falkowski, M.J., Smith, A.M.S., Hudak, A.T., Gessler, P.E., Vierling, L.A., and Crookston, N.L. 2006. Automated estimation of individual conifer tree height and crown diameter via two-dimensional spatial wavelet analysis of lidar data. *Canadian Journal of Remote Sensing*, Vol. 32, No. 2, pp. 153–161.
- Harding, D.J., and Carabajal, C.C. 2005. ICESat waveform measurements of within-footprint topographic relief and vegetation vertical structure. *Geophysical Research Letters*, Vol. 32, L21S10. doi:10.1029/2005GL023471.
- Hemerya, G.E., Savillb, P.S., and Pryor, S.N. 2005. Applications of the crown diameter – stem diameter relationship for different species of broadleaved trees. *Forest Ecology and Management*, Vol. 215, No. 1–3, pp. 285–294.
- Hyypä, J., Kelle, O., Lehtikoinen, M., and Inkinen, M. 2001. A segmentation-based method to retrieve stem volume estimates from 3-D tree height models produced by laser scanners. *IEEE Transactions on Geoscience and Remote Sensing*, Vol. 39, No. 5, pp. 969–975.
- Koch, B., Heyder, U., and Weinacker, H. 2006. Detection of individual tree crowns in airborne lidar data. *Photogrammetric Engineering & Remote Sensing*, Vol. 72, No. 4, pp. 357–363.
- Lefsky, M.A., Harding, D.J., Keller, M., Cohen, W.B., Carabajal, C.C., Espirito-Santo, F.D., Hunter, M.O., and de Oliveira, R. 2005. Estimates of forest canopy height and aboveground biomass using ICESat. *Geophysical Research Letters*, Vol. 32, L22S02. doi:10.1029/2005GL023971.
- Lefsky, M.A., Keller, M., Pang, Y., de Camargo, P., and Hunter, M.O. 2007. Revised method for forest canopy height estimation from Geoscience Laser Altimeter System waveforms. *Journal of Applied Remote Sensing*, Vol. 1, No. 1, 013537. doi:10.1117/12.780665.
- Magnussen, S., and Boudewyn, P. 1998. Derivations of stand heights from airborne laser scanner data with canopy based quantile estimators. *Canadian Journal of Forest Research*, Vol. 28, No. 7, pp. 1016–1031.
- Morsdorf, F., Meier, E., Kötz, B., Itten, K.I., Dobbertin, M., and Allgöwer, B. 2004. LIDAR-based geometric reconstruction of boreal type forest stands at single tree level for forest and wildland fire management. *Remote Sensing of Environment*, Vol. 92, No. 3, pp. 353–362.
- Naesset, E. 2004. Practical large-scale forest stand inventory using small-footprint airborne scanning laser. *Scandinavian Journal of Forest Research*, Vol. 19, No. 2, pp. 164–179.
- Persson, Å., Holmgren, J., and Söderman, U. 2002. Detecting and measuring individual trees using an airborne laser scanner. *Photogrammetric Engineering & Remote Sensing*, Vol. 68, No. 9, pp. 925–932.
- Popescu, S.C., Wynne, R.H., and Nelson, R.F. 2003. Measuring individual tree crown diameter with lidar and assessing its influence on estimating forest volume and biomass. *Canadian Journal of Remote Sensing*, Vol. 29, No. 5, pp. 564–577.
- Pouliot, D.A., King, D.J., and Pitt, D.G. 2005. Development and evaluation of an automated tree detection-delineation algorithm for monitoring regenerating coniferous forests. *Canadian Journal of Forest Research*, Vol. 35, No. 12, pp. 2332–2345.
- Reutebuch, S.E., McGaughey, R.J., Andersen, H.-E., and Carson, W.W. 2003. Accuracy of a high-resolution lidar terrain model under a conifer forest canopy. *Canadian Journal of Remote Sensing*, Vol. 29, No. 5, pp. 527–535.
- Sherrill, K.R., Lefsky, M.A., Bradford, J.B., and Ryan, M.G. 2008. Forest structure estimation and pattern exploration from discrete return lidar in subalpine forests of the Central Rockies. *Canadian Journal of Forest Research*, Vol. 38, No. 8, pp. 2081–2096.
- Sokal, R.R., and Rohlf, F.J. 1981. *Biometry: the principles and practice of statistics in biological research*. 2nd ed. W.H. Freeman, New York. 859 pp.
- Solberg, S., Naesset, E., and Bollandsås, O.M. 2006. Single tree segmentation using airborne laser scanner data in a structurally heterogeneous spruce forest. *Photogrammetric Engineering & Remote Sensing*, Vol. 72, No. 12, pp. 1369–1378.
- Spurr, S.H. 1948. *Aerial photographs in forestry*. Ronald Press, New York. 340 pp.
- Stoker, J., Parrish, J., and Gisclair, D. 2007. *Report of the first national lidar initiative meeting*. US Geological Survey Report Series OF 2007-1189.
- Strahler, A.H., Woodcock, C.E., and Smith, J.A. 1986. On the nature of models in remote sensing. *Remote Sensing of Environment*, Vol. 20, No. 2, pp. 121–139.
- Sun, G., Ranson, K.J., Kimes, D.S., Blair, J.B., and Kovacs, K. 2008. Forest vertical structure from GLAS: An evaluation using LVIS and SRTM data. *Remote Sensing of Environment*, Vol. 112, No. 1, pp. 107–117.
- Waring, K.M., Battles, J.J., and Gonzalez, P. 2006. *Forest carbon and climate change in the Sierra Nevada Mountains of California*. University of California, Berkeley, Calif.
- Yu, X., Hyypä, J., Kaartinen, H., and Maltamo, M. 2004. Automatic detection of harvested trees and determination of forest growth using airborne laser scanning. *Remote Sensing of Environment*, Vol. 90, No. 4, pp. 451–462.
- Zhao, K., and Popescu, S.C. 2007. Hierarchical watershed segmentation of canopy height model for multi-scale forest inventory. In *Proceedings of the ISPRS Working Group Laser Scanning 2007 and SilviLaser 2007*, 12–14 September 2007, Espoo, Finland. Edited by P. Rönholm, H. Hyypä, and J. Hyypä. ISPRS Volume XXXVI, Part 3/W52. International Archives of Photogrammetry and Remote Sensing (ISPRS), ITC, Enschede, The Netherlands, pp. 436–442.
- Zieger, E. 1928. Ermittlung von Bestandesmassen aus Flugbildern mit Hilfe des Hugersoff-Heydeschen Autokartographen. *Mitteilungen aus der Sächsischen forstlichen Versuchsanstalt zu Tharandt*, Vol. 3, pp. 97–127.
- Zwally, H.J., Schutz, B., Abdalati, W., Abshire, J., Bentley, C., Brenner, A., Bufton, J., Dezio, J., Hancock, D., Harding, D., Herring, T., Minster, B., Quinn, K., Palm, S., Spinhrne, J., and Thomas, R. 2002. ICESat's laser measurements of polar ice, atmosphere, ocean, and land. *Journal of Geodynamics*, Vol. 34, No. 3–4, pp. 405–445.